

# A NUMERICAL APPROACH FOR MODELING THE ELECTRIC FIELD AROUND A THREE-DIMENSIONAL VESICLE

EBRAHIM M. KOLAHDOUZ\* AND DAVID SALAC\*†

## Abstract.

The Immersed Interface Method is employed to solve the time-varying electric field equations around a three-dimensional vesicle. To achieve second-order accuracy the jump conditions for the electric potential, up to the second normal derivative, are derived. The trans-membrane potential is determined implicitly as part of the algorithm. To demonstrate the ability of the method sample analytic results are created. Numerical investigations demonstrate that the resulting method is second order accurate even in the presence of discontinuous material properties across the vesicle membrane.

**Key words.** Electric field, vesicle, Immersed Interface Method, trans-membrane potential

**1. Introduction.** The effects of electric fields on biological membranes have been the subjects of recent experimental and theoretical studies. External alternating current (AC) or direct current (DC) electric fields have been proposed as robust methods for a wide range of biotechnological applications and cell manipulation such as electrofusion [1], tissue ablation [2], wound healing [3], and treating tumors [4]. Electric fields can also induce electro-poration in the cell membrane. If the electric field is too strong membrane collapses and cell death may occur [3]. However, a reversible poration process can be achieved through the application of a controlled electric field [2, 5, 6]. Indeed, formation of transient pores are of biotechnological interest for delivering drugs and DNA into living cells [7].

Lipid vesicles form a model system for more complicated non-nucleated biological cells such as red blood cells [8, 9, 10]. Vesicles are also of interest for the technical applications mentioned above. The membrane of a vesicle consists of a bilayer of lipid molecules. It is common to assume that the membrane is impermeable to ions and thus acts as a capacitor [11]. This capacitive property of the interface is very important as it is responsible for the dynamic response of the vesicle and the surrounding electric potential field.

Experiments have recently been reported on the behavior of vesicles subjected to either a DC or AC electric field. Different factors such as the intensity, frequency or duration of exposure to electric fields have been subjects of research in this area [10, 12]. Additionally, recent theoretical works have investigated the electrohydrodynamics of nearly-spherical vesicles. Small-perturbation analysis has been used to generate reduced models in the form of ordinary differential equations [11, 13, 14, 15]. In another work, a boundary integral method was employed to study different equilibrium states of vesicle in the presence of a uniform electric field [16]. However, all these studies are either limited to two dimensional problems or solve simple 3D shapes such as a sphere.

In this work a new numerical method is developed to obtain the time-varying electric and trans-membrane potentials associated with a stationary vesicle. This work is part of a larger effort to understand the general electrohydrodynamics of lipid vesicles. To the authors' knowledge this is the first attempt at calculating the electric potential field by explicitly taking into account the trans-membrane potential for an

---

\*University at Buffalo, Department of Mechanical and Aerospace Engineering, Buffalo, NY, 14260

†Corresponding Author [davidsal@buffalo.edu](mailto:davidsal@buffalo.edu)

arbitrary three-dimensional vesicle. The method presented here is robust and can be applied to any vesicle shape.

This paper is split into the following section: the governing equations will be briefly presented in Section 2. The details of the numerical method and the required electric potential jump conditions are shown in Section 3. In Section 4, sample analytic test cases and numerical convergence results are presented. This is followed by a short conclusion and description of future work in Section 5.

**2. Governing Equations.** Figure (2.1) shows a schematic of a single vesicle exposed to an external electric field. The vesicle is assumed to be made of a charge-free lipid bilayer membrane with capacitance  $C_m$  and conductivity  $G_m$ . It is suspended in a media of conductivity  $s^+$  and dielectric constant  $\epsilon^+$ . The embedded region is assumed to have a different conductivity  $s^-$  and dielectric constant  $\epsilon^-$ .

Application of an electric field causes a redistribution of bulk charge density in both inside and outside of the membrane which decays with a bulk charge relaxation time of [11, 17]

$$\tau_c = \frac{\epsilon^\pm}{s^\pm}. \quad (2.1)$$

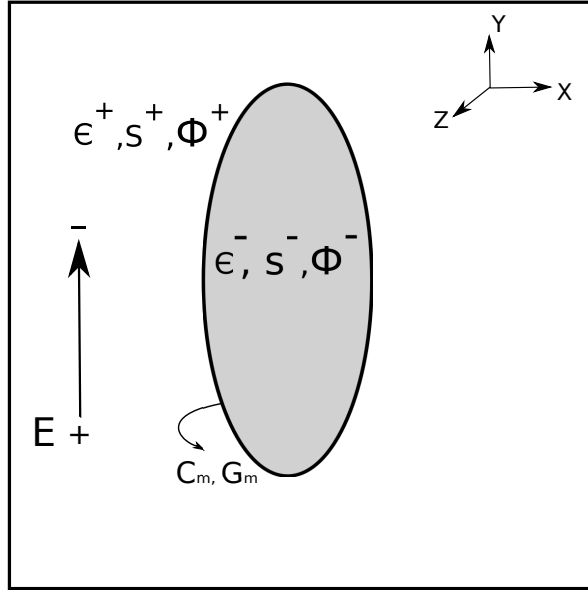


FIG. 2.1. Schematic of a vesicle subjected to external electric field

As there is no local free charge density in the domain, the electric field is irrotational [18],

$$\nabla \times \mathbf{E} = 0. \quad (2.2)$$

The electric field at a point is equal to negative gradient of the electric potential at that point,

$$\mathbf{E}^\pm = -\nabla\Phi^\pm. \quad (2.3)$$

Combining Eq. (2.2) with Eq. (2.3) one can conclude that the electric potential  $\Phi$  is a solution of Laplace equation

$$\nabla^2 \Phi^\pm = 0. \quad (2.4)$$

When an electric field is applied charges will accumulate on both the inner and outer sides of membrane due to the ion impermeability of the lipid bilayer. This turns the membrane into a capacitive interface. However, the membrane capacitor is not charged instantaneously. The relaxation time of the charging process is given by [5, 19]

$$\tau_m = aC_m \left( \frac{1}{s^-} + \frac{1}{2s^+} \right), \quad (2.5)$$

where  $a$  is the radius for a spherical vesicle.

The presence of a capacitive interface results in discontinuity of the potential,

$$\Phi^+ - \Phi^- = -V_m, \quad (2.6)$$

where  $V_m$  is the electric potential jump across the interface and is called the trans-membrane potential. The trans-membrane potential itself can be obtained from the conservation of current density across the membrane [15, 20, 21],

$$C_m \frac{dV_m}{dt} + G_m V_m = \mathbf{n} \cdot \left( s^k \mathbf{E}^\pm + \epsilon^\pm \frac{\partial \mathbf{E}^\pm}{\partial t} \right) + \nabla_s \cdot (\mathbf{v}_s Q^\pm). \quad (2.7)$$

In this relation  $\mathbf{v}_s$  is the interface velocity,  $\mathbf{v}_s Q$  is the convective charge flux on the membrane and  $\mathbf{n}$  is the unit outward normal (pointing from the inner region to the outer region).

For the propose of this problem we ignore the convection of charges associated with the suspending fluid and focus solely on the solution of electric potential. Thus the last term on right-hand side of Eq. (2.7) vanishes. Furthermore, based on the estimation given by Vlahovska *et. al* in Ref. [13] for a typical physiological situation the capacitor charging time is much longer than the bulk charge relaxation time,  $\tau_c \ll \tau_m$ . Therefore the electric field can be assumed to be quasistatic and respond almost instantly to a change in the membrane potential. Under the above-mentioned assumptions, the simplified version of Eq. (2.7) is then expressed as

$$C_m \frac{dV_m}{dt} + G_m V_m = \mathbf{n} \cdot (s^\pm \mathbf{E}^\pm). \quad (2.8)$$

Assuming that the membrane conductance and capacitance have uniform and constant values on the interface, the trans-membrane potential will only depend on changes in the surrounding domain electric potential.

Additionally, the bulk Ohmic current,  $\mathbf{J} = s\mathbf{E}$ , is continuous in normal direction across the membrane. Therefore

$$\mathbf{n} \cdot (\mathbf{J}^+ - \mathbf{J}^-) = \mathbf{n} \cdot (s^+ \mathbf{E}^+ - s^- \mathbf{E}^-) = 0. \quad (2.9)$$

However, there is a discontinuity in the normal component of displacement vector due to induced charges on the membrane

$$\mathbf{n} \cdot (\epsilon^+ \mathbf{E}^+ - \epsilon^- \mathbf{E}^-) = Q, \quad (2.10)$$

where  $Q$  is the induced charge density at the top or bottom of the membrane. This net charge imbalance occurs across the interface due to the difference in physical and electrical properties of the inner and outer regions. It is worth mentioning that  $Q$  is introduced here only for the sake of completeness and is not used in the calculations for the electric potential.

**3. Numerical Method.** First introduced by Leveque and Li [22], the Immersed Interface Method (IIM) is a finite difference method used to solve discontinuous PDE fields across an embedded interface. To produce accurate solutions the jump conditions of the solution are explicitly included in the numerical scheme. This method has been used extensively to solve elliptic problems with interfaces [22, 23, 24] and later was extended to model the Stokes or Navier-Stokes equations with singular forces and discontinuous viscosity [25, 26, 27]. The IIM is also able to handle sharp interfaces with discontinuities and singularities in the coefficients and the solutions [28]. In this section the Immersed Interface Method is briefly described. This is followed by the derivation of the electric potential jump conditions and the specific numerical implementation.

In the Immersed Interface Method grid points can be classified as either regular or irregular points, schematically shown in Fig. 3.1. Regular nodes are defined as those nodes where the interface does not cross the discretization of the PDE. These nodes are treated normally upon discretization, meaning that no modification needs to be applied to the stencil. Irregular nodes, on the other hand, are the ones where the interface crosses the stencil. Modifications need to be made to take into account the discontinuity of the solution at such nodes.

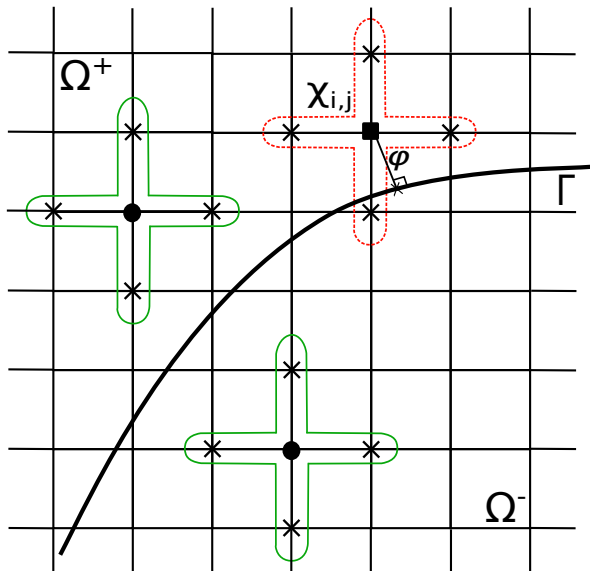


FIG. 3.1. Sample stencils for regular node (circle) and irregular node (square). The stencil in dashed-red crosses the interface and corrections need to be applied. Here  $\varphi$  is the signed distance function to the closest point on the interface from a grid point.

Consider the solution of the electric potential from Eq. (2.4). For the irregular node  $\chi_{i,j}$ , shown in Fig. 3.1, a second-order central finite difference discretization of

the Laplace operator results in

$$\frac{\Phi_{i,j-1}^+ + \Phi_{i-1,j}^+ - 4\Phi_{i,j}^+ + \Phi_{i+1,j}^+ + \Phi_{i,j+1}^+}{h^2} = 0, \quad (3.1)$$

where we have made the assumption that the whole stencil exists in the  $\Omega^+$  domain. However, in reality the point  $\chi_{i,j-1}$  resides in the  $\Omega^-$  domain, not the  $\Omega^+$  domain. To account for this mismatch in the discretization we define a jump in a quantity  $f$  across the interface as

$$[f] = \lim_{\epsilon \rightarrow 0^+} f(\chi_\Gamma + \epsilon \mathbf{n}) - \lim_{\epsilon \rightarrow 0^+} f(\chi_\Gamma - \epsilon \mathbf{n}), \quad (3.2)$$

where  $\chi_\Gamma$  is the closest-point location on the interface to the grid point  $\chi$  and  $\mathbf{n}$  is the outward normal vector. Quantities on the interface can be defined based on the direction from which the interface is approached,

$$f^- = \lim_{\epsilon \rightarrow 0^+} f(\chi_\Gamma - \epsilon \mathbf{n}), \quad (3.3)$$

$$f^+ = \lim_{\epsilon \rightarrow 0^+} f(\chi_\Gamma + \epsilon \mathbf{n}). \quad (3.4)$$

Assume that the physics of the problem provides enough information to derive the jumps in the solution,  $[\Phi]$ , the first normal derivative,  $[\partial\Phi/\partial n]$ , and the second normal derivative,  $[\partial^2\Phi/\partial n^2]$ , on the interface. Consequently the jump can be extended to a grid point by applying a Taylor Series expansion in the normal direction about the closest point location [27, 29],

$$[\Phi]_{i,j} = [\Phi] + \varphi_{i,j} \left[ \frac{\partial\Phi}{\partial n} \right] + \frac{\varphi_{i,j}^2}{2} \left[ \frac{\partial^2\Phi}{\partial n^2} \right] + O(h^3), \quad (3.5)$$

where  $\varphi_{i,j}$  is the signed distance function from the grid point  $\chi_{i,j}$  to the corresponding location on the interface. By extending the solution jumps from the interface to the grid points it can be written that  $\Phi_{i,j-1}^- = \Phi_{i,j-1}^+ - [\Phi]_{i,j-1}$ . Using this expression in Eq. (3.1) results in the corrected discretization,

$$\frac{\Phi_{i,j-1}^- + \Phi_{i-1,j}^+ - 4\Phi_{i,j}^+ + \Phi_{i+1,j}^+ + \Phi_{i,j+1}^+}{h^2} + \frac{[\Phi]_{i,j-1}}{h^2} = 0. \quad (3.6)$$

The known jump value,  $[\Phi]_{i,j-1}$ , is obtained from Eq. (3.5) and can be moved to the right-hand side of the linear system as an explicit correction term,

$$\frac{\Phi_{i,j-1}^- + \Phi_{i-1,j}^+ - 4\Phi_{i,j}^+ + \Phi_{i+1,j}^+ + \Phi_{i,j+1}^+}{h^2} = C_{i,j}, \quad (3.7)$$

where  $C_{i,j} = -[\Phi]_{i,j-1}/h^2$  is the total correction needed to discretize the Laplace operator over the irregular node  $\chi_{i,j}$ . The extension of this method to irregular nodes on either side of the interface and to three-dimensional systems is straight-forward.

**3.1. Electric Potential Jump Conditions.** Now consider the discretization of the entire computational domain. The governing equation for the electric potential can be written over the entire domain as

$$\nabla^2\Phi = C, \quad (3.8)$$

where the total correction  $C$  is only non zero for irregular nodes. To be able to calculate this correction, the jump conditions for  $\Phi$  and it's normal derivatives on the interface need to be derived. The jump in electric potential is easily obtained from Eq. (2.6) as

$$[\Phi] = -V_m. \quad (3.9)$$

The trans-membrane potential,  $V_m$ , is a time-varying quantity with the evolution being described by Eq. (2.8). To discretize this equation, first make use of Eq. (2.3) to express the electric field in terms of the electric potential. This results in the expression

$$C_m \frac{dV_m}{dt} + G_m V_m = -s^\pm \frac{\partial \Phi^\pm}{\partial n}. \quad (3.10)$$

Using a first-order in time discretization and treating the term  $G_m V_m$  implicitly result in

$$C_m \frac{V_m^{n+1} - V_m^n}{\Delta t} + G_m V_m^{n+1} = -s^\pm \frac{\partial \Phi^\pm}{\partial n}. \quad (3.11)$$

Solving for the trans-membrane potential  $V_m^{n+1}$  gives the jump of the electric potential across the interface,

$$[\Phi] = -V_m^{n+1} = \frac{1}{C_m + \Delta t G_m} (\Delta t s^\pm \frac{\partial \Phi^\pm}{\partial n} - C_m V_m^n). \quad (3.12)$$

To derive the jump condition for the first normal derivative of electric potential utilize the continuity of current density across the interface, Eq. (2.9):

$$0 = s^+ \frac{\partial \Phi^+}{\partial n} - s^- \frac{\partial \Phi^-}{\partial n}, \quad (3.13)$$

$$0 = s^+ \frac{\partial \Phi^+}{\partial n} - s^- \frac{\partial \Phi^-}{\partial n} + s^- \frac{\partial \Phi^+}{\partial n} - s^- \frac{\partial \Phi^+}{\partial n}, \quad (3.14)$$

$$0 = (s^+ - s^-) \frac{\partial \Phi^+}{\partial n} + s^- \left( \frac{\partial \Phi^+}{\partial n} - \frac{\partial \Phi^-}{\partial n} \right), \quad (3.15)$$

$$0 = [s] \frac{\partial \Phi^+}{\partial n} + s^- \left[ \frac{\partial \Phi}{\partial n} \right]. \quad (3.16)$$

Similarly it can be shown that

$$0 = [s] \frac{\partial \Phi^-}{\partial n} + s^+ \left[ \frac{\partial \Phi}{\partial n} \right]. \quad (3.17)$$

Solving for the jump in the normal electric field yields

$$\left[ \frac{\partial \Phi}{\partial n} \right] = -\frac{[s]}{s^+} \frac{\partial \Phi^-}{\partial n} = -\frac{[s]}{s^-} \frac{\partial \Phi^+}{\partial n}, \quad (3.18)$$

For the jump in the second normal derivative, start with the relation between the Laplacian and the surface Laplacian of an arbitrary scalar function

$$\nabla^2 \Phi = \nabla_s^2 \Phi + H \frac{\partial \Phi}{\partial n} + \frac{\partial^2 \Phi}{\partial n^2}, \quad (3.19)$$

where  $\nabla_s^2$  is the surface Laplacian and  $H$  is the total curvature. Applying the jump operator to Eq. (3.19) results in

$$[\nabla^2\Phi] = [\nabla_s^2\Phi] + H \left[ \frac{\partial\Phi}{\partial n} \right] + \left[ \frac{\partial^2\Phi}{\partial n^2} \right]. \quad (3.20)$$

Previous work has shown that the jump condition commutes with differentiation,  $[\nabla_s^2\Phi] = \nabla_s^2[\Phi]$ , see Ref. [30]. Also note that from Eq. (2.4) the jump in the Laplacian of the electric potential is zero,  $[\nabla^2\Phi] = 0$ . It is thus possible to write the jump in the second normal derivative as

$$\left[ \frac{\partial^2\Phi}{\partial n^2} \right] = -\nabla_s^2[\Phi] - H \left[ \frac{\partial\Phi}{\partial n} \right], \quad (3.21)$$

where the expressions for  $[\Phi]$  and  $[\partial\Phi/\partial n]$  are given in Eqs. (3.12) and (3.18).

**3.2. Numerical Implementation.** To proceed with the numerical algorithm the normal electric field in either the  $\Omega^-$  or  $\Omega^+$  is introduced as a new variable,

$$r = \frac{\partial\Phi^\alpha}{\partial n}, \quad (3.22)$$

where the superscript  $\alpha$  represents the sign of the domain with lower conductivity. With this new definition, the complete set of jump conditions can be rewritten as

$$[\Phi] = \frac{1}{C_m + \Delta t G_m} (\Delta t s^\alpha r - C_m V_m^n), \quad (3.23)$$

$$\left[ \frac{\partial\Phi}{\partial n} \right] = -\frac{[s]}{s^{-\alpha}} r, \quad (3.24)$$

$$\left[ \frac{\partial^2\Phi}{\partial n^2} \right] = \nabla_s^2 \left( \frac{1}{C_m + \Delta t G_m} (C_m V_m^n - \Delta t s^\alpha r) \right) + H \frac{[s]}{s^{-\alpha}} r, \quad (3.25)$$

In this presentation of the jump conditions the value  $s^{-\alpha}$  in Eq. (3.24) represents the value from the region with the higher conductivity. If the normal electric field,  $r$ , is known then the jump conditions can be calculated. This allows for the determination of the electric potential through the solution of Eq. (3.8).

All the jump conditions given in (3.23)-(3.25) are linear. Hence, all the IIM corrections will be linear near the interface. Therefore, the resulting linear system from the field equation in Eq. (3.8) can be written in operator form as

$$\mathbf{L}\Phi = \mathbf{C}, \quad (3.26)$$

where  $\mathbf{L}$  is the Laplacian operator and  $\mathbf{C}$  is the vector containing the required corrections. The total correction  $\mathbf{C}$  can be split into corrections due to  $\mathbf{r}$  and  $\mathbf{V}_m^n$ ,

$$\mathbf{C} = \mathbf{A}_0 \mathbf{r} + \mathbf{B}_0 \mathbf{V}_m^n \quad (3.27)$$

where  $\mathbf{A}_0$  and  $\mathbf{B}_0$  are also linear operators, and  $\mathbf{r}$  and  $\mathbf{V}_m^n$  contain the normal electric field and the previous time step's trans-membrane potential, both defined on the interface.

By combining (3.27) and (3.26), it is possible to solve for electric potential,

$$\Phi = \mathbf{L}^{-1} \mathbf{A}_0 \mathbf{r} + \mathbf{L}^{-1} \mathbf{B}_0 \mathbf{V}_m^n. \quad (3.28)$$

Let  $M_n$  be the one-sided normal derivative operator such that  $M_n \Phi = r$ . It is now possible to write

$$M_n \Phi = r = M_n L^{-1} A_0 r + M_n L^{-1} B_0 V_m^n. \quad (3.29)$$

Equation (3.29) shows that the normal electric field,  $r$ , has two linear contributions. These is a contribution from the trans-membrane potential at a previous time and a contribution from the normal electric field itself. As the quantity  $V_m^n$  is known that particular contribution can be explicitly calculated as

$$r_0 = M_n L^{-1} B_0 V_m^n, \quad (3.30)$$

which is simply the solution of the electric potential field using only the contribution to the jump conditions from  $V_m^n$  (*i.e.* the jump conditions in Eqs. (3.23)-(3.25) are computed with  $r = 0$ ). This electric potential solution is then projected onto the normal electric field space through the  $M_n$  operator.

The second contribution is from the still-unknown normal electric field,  $r$ . This contribution, though, can be written as  $M_n L^{-1} A_0 r = A r$ , where  $A r$  is the solution of the electric potential projected onto the normal electric field space by only considering the  $r$  contributions to the jump conditions, Eqs. (3.23)-(3.25).

Using this simplified notation it can be stated that  $r$  is the solution to the following linear system,

$$(A - I)r = -r_0. \quad (3.31)$$

As this linear system can not be written in explicit form, a matrix-free iterative linear system solution method is needed to obtain the solution. The quantity  $r$  is only defined on the interface and is thus a lower dimension than the computational domain. Therefore a solver such as GMRES proves to be an excellent choice.

**3.3. The Numerical Algorithm.** The algorithm to solve Eq. (3.31) can be written as:

**Step I:**

Solve for the electric potential field using only the known  $V_m^n$ :  
 $\Phi_0 = L^{-1} B_0 V_m^n$  with the physical boundary conditions.

**Step II:**

Compute the constant contribution to the normal electric field as  
 $r_0 = M_n \Phi_0$ .

**Step III:**

Utilize a matrix-free iterative linear solver to solve Eq. (3.31) for  $r$ . Each matrix-vector product  $(A - I)r$  requires the following steps:

**Step 1:** Solve for the electric potential using the iterative linear system solver provided values for  $r$ :  $\Phi_r = L^{-1} A_0 r$  with uniform boundary conditions of  $\Phi_r|_{bc} = 0$ .

**Step 2:** Calculate the normal electric field as  $A r = M_n \Phi_r$ .

**Step 3:** Return the quantity  $(A - I)r$  as the matrix-vector product.



**Step IV:**

The electric potential field in the computational domain is  $\Phi = \Phi_0 + \Phi_r$ .

**Step V:**

The new trans-membrane potential is

$$\mathbf{V}_m^{n+1} = \frac{-1}{C_m + \Delta t G_m} (\Delta t s^\alpha \mathbf{r} - C_m V_m^n). \quad (3.32)$$

**4. Results.** In this section the convergence, accuracy and robustness of the method is investigated through various numerical experiments. In particular, convergence results are presented demonstrating the accuracy of the method. Both single time-step and multi-time-step convergence are considered. Additionally, the number of GMRES iterations needed to obtain convergence is also investigated. Finally, a qualitative study is presented to illustrate the change of domain and trans-membrane potentials over time for an ellipsoidal vesicle in the presence of a uniform DC electric field.

For all the cases considered, the physical domain is a  $[-2, 2]^3$  cube. The conductivities of the regions are set to be  $s^- = 50.0$  in the inner region and  $s^+ = 1.0$  in the outer region. For simplicity, the membrane capacitance and conductance are both set to 1.0. The relative convergence tolerance for all iterative linear system solvers is set to  $10^{-5}$ .

**4.1. Single Time Step Convergence.** Consider a spherical vesicle of radius one centered at the origin. To examine the accuracy of the underlying discretization of the problem, a well-behaved time-independent solution of the electric potential field is developed. This analytic solution was created to satisfy the field equations and all jump conditions. The analytic solutions for the electric potential in the domain ( $\Phi$ ) and potential jump ( $V_m$ ) on the interface are taken to be

$$\Phi^- = \frac{\exp(\sqrt{2}z) \sin(x) \cos(y)}{s^-} + 1.0, \quad (4.1)$$

$$\Phi^+ = \exp(\sqrt{2}z) \sin(x) \cos(y), \quad (4.2)$$

$$V_m = \frac{\exp(\sqrt{2}z) \sin(x) \cos(y)}{s^-} + 1.0 - \exp(\sqrt{2}z) \sin(x) \cos(y). \quad (4.3)$$

For a grid spacing of  $h$  this system is solved over a single time step equal to  $\Delta t = 2h^2$  using Dirichlet boundary conditions of  $\Phi_{bc} = \phi^+$ . It is thus necessary to explicitly define the trans-membrane potential at the previous time-step. Using the first-order discretization in Eq. (3.11) the trans-membrane potential at the previous time-step is can be calculated by analytically taking a step backwards in time, resulting in

$$V_0 = \frac{C_m + \Delta t G_m}{-C_m} \left( \frac{\exp(\sqrt{2}z) \sin(x) \cos(y)}{s^-} + 1.0 - \exp(\sqrt{2}z) \sin(x) \cos(y) \right) \quad (4.4)$$

$$- \Delta t s^+ \exp(\sqrt{2}z) \left( \frac{x \cos(x) \cos(y) - y \sin(x) \sin(y) + z \sqrt{2} \sin(x) \cos(y)}{\sqrt{x^2 + y^2 + z^2}} \right). \quad (4.5)$$

TABLE 4.1

Domain Potential ( $\Phi$ ) error for a sphere in the domain  $[-2, 2]^3$  for the case of single time step.

$N$	$L_2$	Order	$L_\infty$	Order
33	$9.26 \times 10^{-6}$	-	$8.25 \times 10^{-3}$	-
65	$8.57 \times 10^{-7}$	3.43	$2.08 \times 10^{-3}$	1.98
129	$7.72 \times 10^{-8}$	3.47	$5.21 \times 10^{-4}$	1.99
257	$6.88 \times 10^{-9}$	3.48	$1.29 \times 10^{-4}$	2.01

TABLE 4.2

Trans-membrane potential ( $V_m$ ) error for a sphere on the domain  $[-2, 2]^3$  for the case of a single time step.

$N$	$L_2$	Order	$L_\infty$	Order
33	$4.03 \times 10^{-7}$	-	$5.96 \times 10^{-4}$	-
65	$1.38 \times 10^{-8}$	3.04	$8.47 \times 10^{-5}$	2.81
129	$4.54 \times 10^{-10}$	3.07	$1.18 \times 10^{-5}$	2.84
257	$2.34 \times 10^{-12}$	3.39	$2.46 \times 10^{-7}$	2.26

The resulting errors are shown in Tables (4.1) and (4.2). Overall the domain electric potential observes second-order convergence in the  $L_\infty$ -norm error while the trans-membrane potential has a slightly higher accuracy. This matches the underlying second-order finite difference approximation of the spatial derivatives.

It is important to note that the extension of the jumps need to be calculated to third order accuracy to ensure that irregular nodes have a local truncation error of  $O(h)$ . Despite this lower local truncation error, the overall method will retain the second-order accuracy of the underlying discretization. If the second-normal derivative jump is not taken into account, the local truncation error for irregular nodes will be reduced to  $O(1)$  and the overall scheme would only be first-order [23, 27, 31].

**4.2. Time-Varying Convergence.** In this example the convergence for a time-varying electric potential field is demonstrated. The exact solution of the electric potential and trans-membrane potential are taken to be

$$\Phi^- = \frac{\exp(-t)}{s^-} (3x^2 - y^2 - 2z^2), \quad (4.6)$$

$$\Phi^+ = \exp(-t) (3x^2 - y^2 - 2z^2), \quad (4.7)$$

$$V_m = \frac{\exp(-t)}{s^-} (3x^2 - y^2 - 2z^2) - \exp(-t) (3x^2 - y^2 - 2z^2). \quad (4.8)$$

The initial trans-membrane potential is given as

$$V_0 = V_m(t=0) = \frac{(3x^2 - y^2 - 2z^2)}{s^-} - (3x^2 - y^2 - 2z^2). \quad (4.9)$$

As before Dirichlet boundary conditions are imposed.

As Eq. (3.10) is discretized using a first order Euler method the time step is scaled as  $h^2$  to match the spatial discretization. The errors at a final time of 0.375 are shown in Tables (4.3) and (4.4). As in the single time-step case we observe second-order accuracy in the  $L_\infty$ -norm and third-order accuracy in the  $L_2$ -norm for both the domain electric potential and trans-membrane potential.

TABLE 4.3

Domain Potential ( $\Phi$ ) error for a sphere on the domain  $[-2, 2]^3$  for a time-varying function. The time step is  $\Delta t = 2h^2$  while the final time is  $T_{final} = 0.375$ .

$N$	$L_2$	Order	$L_\infty$	Order
33	$2.53 \times 10^{-6}$	-	$4.52 \times 10^{-3}$	-
65	$2.39 \times 10^{-7}$	3.40	$1.19 \times 10^{-3}$	1.98
129	$2.26 \times 10^{-8}$	3.40	$3.15 \times 10^{-4}$	1.99
257	$1.98 \times 10^{-9}$	3.51	$8.08 \times 10^{-5}$	2.01

TABLE 4.4

Trans-membrane potential ( $V_m$ ) error for a sphere on the domain  $[-2, 2]^3$  for a time-varying function. The time step is  $\Delta t = 2h^2$  while the final time is  $T_{final} = 0.375$ .

$N$	$L_2$	Order	$L_\infty$	Order
33	$5.38 \times 10^{-6}$	-	$5.81 \times 10^{-3}$	-
65	$3.56 \times 10^{-7}$	3.92	$1.36 \times 10^{-3}$	2.81
129	$2.31 \times 10^{-8}$	3.94	$3.34 \times 10^{-4}$	2.84
257	$1.48 \times 10^{-9}$	3.96	$8.56 \times 10^{-5}$	2.26

One possible limitation of the method is the number of GMRES iterations. As each matrix-vector product requires the solution of a linear system, a large number of GMRES iterations would result in an extremely computationally expensive method. In Fig (4.1) the number of GMRES iterations versus the time step for the example in this section are provided. In all cases the number of GMRES iterations remains between three and six, irregardless of the grid size. While this is not a complete test it appears that the number of GMRES iterations slightly decreases as the mesh size decreases.

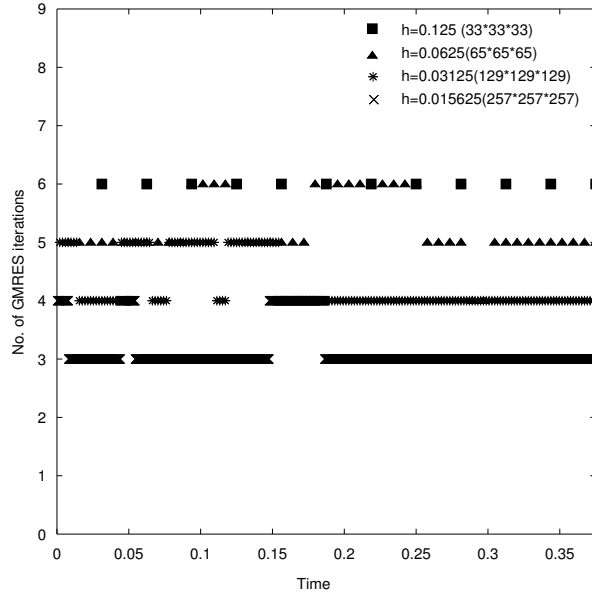


FIG. 4.1. The number of GMRES iterations versus time for different mesh sizes.

**4.3. Ellipsoidal vesicle in presence of uniform DC field.** To provide more physical insight into the application of the method developed here a stationary ellipsoidal vesicle subjected to a uniform DC electric field is considered. It should be noted that the scope of this paper is solely to find the solution for the electric potential for a given three-dimensional vesicle shape and thus the vesicle shape is static.

The vesicle is given by the level set equation

$$\varphi = \left(\frac{x}{a}\right)^2 + \left(\frac{y}{b}\right)^2 + \left(\frac{z}{c}\right)^2 - 1, \quad (4.10)$$

with  $a = c = 0.5$  and  $b = 1.2$ . Dirichlet boundary conditions of  $\Phi(x, 2, z) = 2$  and  $\Phi(x, -2, z) = 0$  are applied while periodicity is assumed in the  $x$ - and  $z$ - directions, see Fig. 4.2. At  $t = 0$  the domain electric potential is assumed to be continuous and thus the trans-membrane potential is equal to zero,  $V_m(t = 0) = 0$ . Over time the membrane will fully charge and thus the trans-membrane potential will obtain a steady solution. Due to the high inner conductivity it should also be expected the electric field in the inner region to be dramatically smaller than the outer region.

The time evolution of the trans-membrane potential is shown in Fig. 4.3. Due to the use of spatially constant membrane conductivity and permittivity the trans-membrane potential evolves to have a constant gradient along the  $y$ -direction. This can also be seen when investigating the electric potential on the  $z = 0$  plane, Fig. 4.4. At time  $t = 0$  the electric potential is continuous in the computational domain. As the membrane charges the sharp discontinuity begins to become evident. At steady-state, demonstrated here at time  $t = 0.3$ , the electric field in the inner domain,  $\Omega^-$ , is clearly small while the outer domain,  $\Omega^+$ , is much larger.

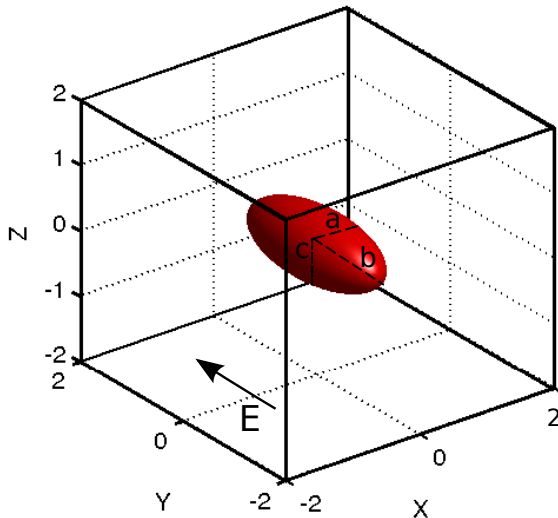


FIG. 4.2. Schematic of ellipsoid shape vesicle in the presence of uniform electric field

**5. Concluding remarks.** For the first time a numerical method is developed to solve both for the electric potential field and trans-membrane potential associated with a three-dimensional vesicle. The jump conditions for the electric potential field

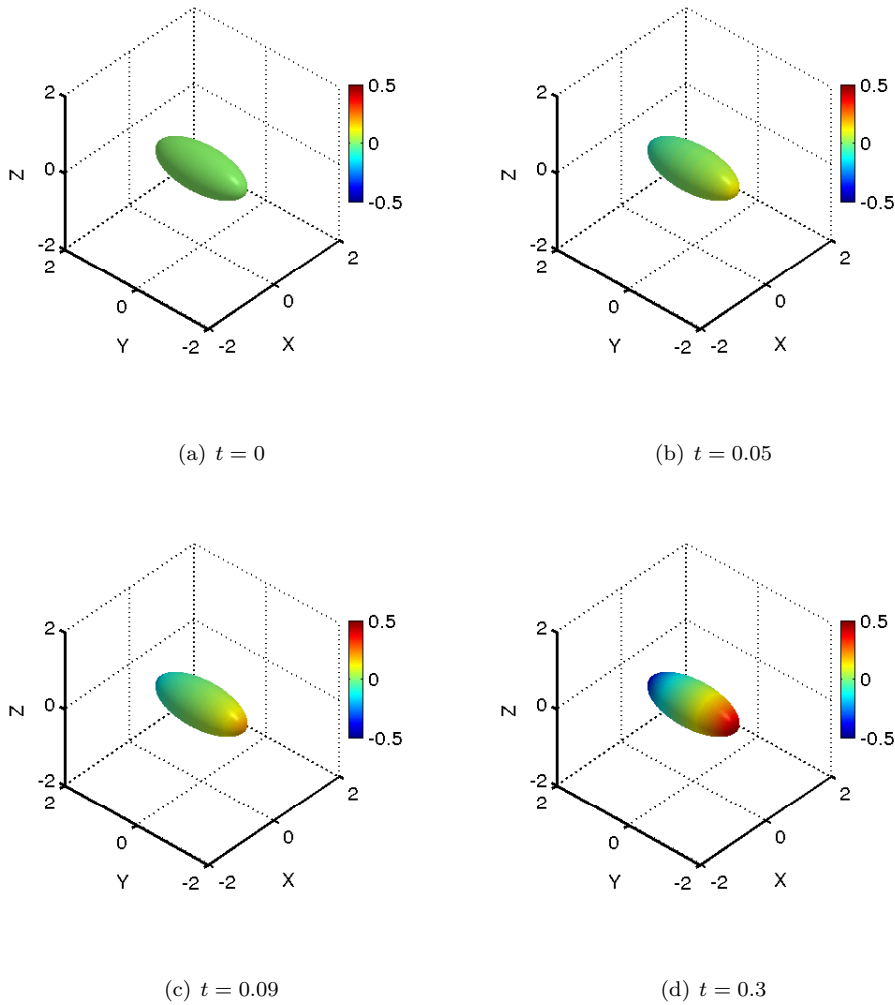


FIG. 4.3. *Trans-membrane potential on the ellipsoid surface. The grid spacing is  $h = 0.03125$  and the time step is  $\Delta t = 0.002$*

are determined and utilized in an Immersed Interface Method to obtain accurate electric potential field solutions. The accuracy of the method is tested for two sets of analytic solutions and the results show second order accuracy for both the domain and trans-membrane potentials. Moreover, a qualitative study is performed to compute the domain and trans-membrane potentials for an ellipsoidal vesicle subjected to DC electric field. The jump in the solution due to discontinuous conductivity between the two regions is effectively captured. Also the change of trans-membrane potential over time is consistent with the direction of the applied electric field.

Future work will see this method applied to investigate the electrohydrodynamic response of lipid vesicles. As the electric field can respond much faster than the vesicle membrane or the fluid field, it can be considered as quasi-static. It is thus possible to directly couple the work here with a multi-phase fluid flow solver and accurate

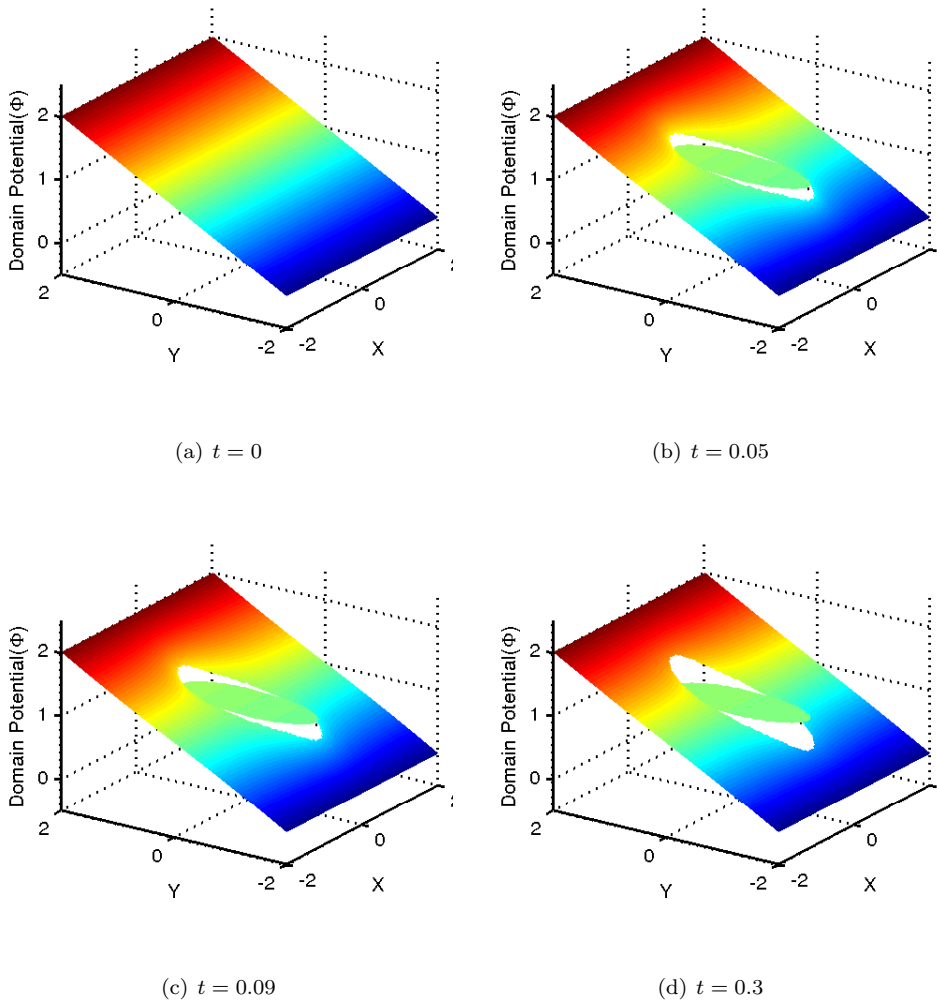


FIG. 4.4. Domain potential distribution on the  $z = 0$  plane. The grid spacing is  $h = 0.03125$  and the time step is  $\Delta t = 0.002$

interface tracking techniques to model the electrohydrodynamic response of vesicles. This is an area of ongoing research and will be addressed in the future.

## REFERENCES

- [1] A. E. S. Donald C. Chang , Bruce M. Chassy , James A. Saunders, Guide to electroporation and electrofusion, Academic Press, New York, 1992.
- [2] B. Rubinsky, G. Onik, P. Mikus, Irreversible electroporation: a new ablation modality–clinical implications, *Technology in cancer research & treatment* 6 (1) (2007) 37–48.
- [3] C. R. Keese, J. Wegener, S. R. Walker, I. Giaever, Electrical wound-healing assay for cells in vitro, *Proceedings of the National Academy of Sciences of the United States of America* 101 (6) (2004) 1554–9.
- [4] R. Heller, R. Gilbert, M. Jaroszeski, Clinical applications of electrochemotherapy, *Advanced drug delivery reviews* 35 (1) (1999) 119–129.
- [5] K. Kinoshita, I. Ashikawa, N. Saita, H. Yoshimura, H. Itoh, K. Nagayama, a. Ikegami, Electroporation of cell membrane visualized under a pulsed-laser fluorescence microscope, *Biophysical journal* 53 (6) (1988) 1015–9.
- [6] W. Krassowska, P. D. Filev, Modeling electroporation in a single cell, *Biophysical journal* 92 (2) (2007) 404–17.
- [7] T. Y. Tsong, Electroporation of cell membranes., *Biophysical journal* 60 (2) (1991) 297–306.
- [8] R. Dimova, N. Bezlyepkina, M. D. Jordö, R. L. Knorr, K. a. Riske, M. Staykova, P. M. Vlahovska, T. Yamamoto, P. Yang, R. Lipowsky, Vesicles in electric fields: Some novel aspects of membrane behavior, *Soft Matter* 5 (17) (2009) 3201.
- [9] R. Dimova, K. a. Riske, S. Aranda, N. Bezlyepkina, R. L. Knorr, R. Lipowsky, Giant vesicles in electric fields, *Soft Matter* 3 (7) (2007) 817.
- [10] K. A. Riske, R. Dimova, Electro-deformation and poration of giant vesicles viewed with high temporal resolution, *Biophysical journal* 88 (2) (2005) 1143–55.
- [11] J. T. Schwalbe, P. M. Vlahovska, M. J. Miksis, Vesicle electrohydrodynamics, *Physical Review E* 83 (4) (2011) 046309.
- [12] K. A. Riske, R. Dimova, Electric pulses induce cylindrical deformations on giant vesicles in salt solutions, *Biophysical journal* 91 (5) (2006) 1778–86.
- [13] P. M. Vlahovska, R. S. Gracià, S. Aranda-Espinoza, R. Dimova, Electrohydrodynamic model of vesicle deformation in alternating electric fields, *Biophysical journal* 96 (12) (2009) 4789–803.
- [14] J. T. Schwalbe, P. M. Vlahovska, M. J. Miksis, Lipid membrane instability driven by capacitive charging, *Physics of Fluids* 23 (4) (2011) 041701.
- [15] J. Seiwert, M. J. Miksis, P. M. Vlahovska, Stability of biomimetic membranes in DC electric fields, *Journal of Fluid Mechanics* 706 (2012) 58–70.
- [16] L. C. McConnell, M. J. Miksis, P. M. Vlahovska, Vesicle electrohydrodynamics in DC electric fields, *IMA Journal of Applied Mathematics* 78 (4) (2013) 797–817.
- [17] J. R. Melcher, G. I. Taylor, Electrohydrodynamics: A review of the role of interfacial shear stresses, *Annual Review of Fluid Mechanics* 1 (1) (1969) 111–146.
- [18] D. A. Saville, Electrohydrodynamics: The Taylor-Melcher leaky dielectric model, *Annual Review of Fluid Mechanics* 29 (1962) (1997) 27–64.
- [19] M. Hibino, M. Shigemori, H. Itoh, K. Kinoshita, Membrane conductance of an electroporated cell analyzed by submicrosecond imaging of transmembrane potential Pulsed-laser fluorescence, *Biophysical journal* 59 (January) (1991) 209–220.
- [20] K. A. DeBruin, W. Krassowska, Modeling electroporation in a single cell. I. Effects Of field strength and rest potential., *Biophysical journal* 77 (3) (1999) 1213–24.
- [21] J. Seiwert, P. M. Vlahovska, Instability of a fluctuating membrane driven by an ac electric field, *Physical Review E* 87 (2) (2013) 022713.
- [22] R. J. LeVeque, Z. Li, The immersed interface method for elliptic equations with discontinuous coefficients and singular sources, *SIAM Journal on Numerical Analysis* 31 (4) (1994) 1019–1044.
- [23] R. J. LeVeque, Z. Li, Immersed interface methods for Stokes flow with elastic boundaries or surface tension, *SIAM Journal on Scientific Computing* 18 (3) (1997) 709–735.
- [24] Z. Li, A fast iterative algorithm for elliptic interface problems, *SIAM Journal on Numerical Analysis* 35 (1) (1998) 230–254.
- [25] Z. Li, M.-C. Lai, The immersed interface method for the navier–stokes equations with singular forces, *Journal of Computational Physics* 171 (2) (2001) 822–842.
- [26] D. Le, B. Khoo, J. Peraire, An immersed interface method for viscous incompressible flows involving rigid and flexible boundaries, *Journal of Computational Physics* 220 (1) (2006) 109–138.
- [27] P. Gera, D. Salac, The three-dimensional jump conditions for the stokes equations with discontinuous viscosity, singular forces and an incompressible interface [arXiv:arXiv:1309.1728v1](https://arxiv.org/abs/1309.1728v1).

- [28] Z. Li, An overview of the immersed interface method, *Taiwanese Journal of Mathematics* 7 (1) (2003) 1–49.
- [29] M.-C. Lai, H.-C. Tseng, A simple implementation of the immersed interface methods for Stokes flows with singular forces, *Computers & Fluids* 37 (2) (2008) 99–106.
- [30] S. Xu, Z. J. Wang, Systematic derivation of jump conditions for the immersed interface method in three-dimensional flow simulation, *SIAM Journal on Scientific Computing* 27 (6) (2006) 1948–1980.
- [31] L. Adams, Z. Li, The immersed interface/multigrid methods for interface problems, *SIAM Journal on Scientific Computing* 24 (2) (2002) 463–479.